

Magnetic Properties for the One-Dimensional Multicomponent Spin-Gap System

Akira Kawaguchi, Tatsuya Fujii and Norio Kawakami

Department of Applied Physics, Osaka University, Suita, Osaka 565-0871, Japan

(October 30, 2018)

Magnetic properties for the one-dimensional multicomponent quantum spin system with the excitation gap are studied based on the integrable spin model introduced by Bariev *et al.* By exactly computing the magnetization, we show how the characteristic structure with plateaus and cusps appears in the magnetization process. To study low-energy dynamics of the system, we apply the finite-size scaling analysis to the excitation spectrum, and thereby evaluate the power-law exponent as well as the enhancement factor for the low-temperature NMR relaxation rate $1/T_1$. We discuss the critical properties of $1/T_1$ around plateaus and cusps in the magnetization curve.

PACS numbers: 75.10.Jm, 75.40.Gb

I. INTRODUCTION

Quantum phase transitions of one-dimensional (1D) spin systems in a magnetic field have attracted much interest recently. One of the most remarkable phenomena is the plateau formation in the magnetization process,^{1–5} which is caused by a field-induced spin gap. Also, the closure of the spin gap in the Haldane system and the ladder system by the magnetic field has been providing an interesting subject,^{6,7} which shares common important physics with the plateau formation.

Another hot topic in 1D spin systems has been concerned with the multicomponent version of the spin model or the spin-orbital model, since it was recognized that the orbital degrees of freedom give rise to a variety of interesting phenomena. Experimentally, 1D correlated electron systems at quarter-filling, such as $\text{Na}_2\text{Ti}_2\text{Sb}_2\text{O}_8$ and NaV_2O_5 ,⁹ have been studied extensively, for which the orbital degrees of freedom play an important role.^{10–12} In this context, the 1D $\text{SU}(4)$ massless spin model has been studied numerically^{13,14} and analytically^{15–19} as the simplest spin-orbital model, and this type of analysis has been extended to a perturbed $\text{SU}(4)$ model to study the gap formation.^{20–24}

According to the above studies, it may be interesting to investigate how the orbital degeneracy affects field-induced quantum phase transitions such as the plateau formation in 1D spin systems. To address this problem, in this paper, we investigate static and dynamical properties for the 1D multicomponent spin-gap system in a magnetic field. For this purpose, we employ the 1D multicomponent anisotropic Heisenberg model, which was exactly solved by Bariev *et al.*²⁵ In particular, we focus our attention on the critical regions where the spin-gap

disappears, or the magnetization plateau (or cusp) is generated in the presence of a magnetic field. To study the low-energy dynamics of the system, we further discuss the NMR relaxation rate $1/T_1$ around the field-induced quantum phase transitions at low temperatures.^{26–32}

This paper is organized as follows. In Sect.II, we exactly calculate the magnetization curve for the 1D anisotropic Heisenberg model,²⁵ and determine the magnetic phase diagram. We clarify how the plateaus and cusps are generated in the magnetization curve. In Sect.III, by exploiting finite-size scaling techniques³³ we discuss the low-temperature behavior of the NMR relaxation rate $1/T_1$ with the emphasis on the critical properties around plateaus and cusps. It is shown that the enhancement factor plays a significant role for $1/T_1$ around such critical regions. A brief summary is given in Sect.IV.

II. PLATEAUS AND CUSPS IN THE MAGNETIZATION

In this section, we study the magnetization process for the anisotropic Heisenberg model with a two-band structure in 1D, which is defined by the deformed version of the $\text{SU}(4)$ Heisenberg model,²⁵

$$\mathcal{H}_0 = J \sum_i \sum_{m \neq m'} \{c_{im}^\dagger c_{im'} c_{i+1m'}^\dagger c_{i+1m}\} - \exp[\text{sign}(m' - m)\Phi] n_{im} n_{i+1m'}, \quad (1)$$

where it is prohibited that more than one electron occupies each site. Here, c_{im}^\dagger is the creation operator for electrons with spin (\uparrow, \downarrow) and orbital (1, 2) degrees of freedom. We shall use the indices $m = 1, 2, 3, 4$ for these four states so that the corresponding number of electrons N_m should satisfy, $N_1 \geq N_2 \geq N_3 \geq N_4$ in a magnetic field. In the isotropic case ($\Phi = 0$), the Hamiltonian (1) is reduced to the $\text{SU}(4)$ massless Heisenberg model,¹⁵ whereas for any other cases it is massive for all excitations at zero magnetic field.²⁵ Although the above integrable model is rather special in its appearance, we think that its characteristic behavior in a magnetic field, such as the formation of plateaus and cusps, should capture some generic properties expected for multicomponent spin-gap models in 1D.

The exact solution of the model (1) with periodic boundary conditions was obtained by Bariev *et al.*²⁵ The Bethe equations obtained for rapidities $\lambda_j^{(\alpha)}$ ($\alpha = 1, 2, 3$) read^{25,34},

$$2\pi I_j^\alpha - N\Theta_1(\lambda_j^\alpha)\delta_{\alpha 1} = \sum_{s=\pm 1} \sum_{i=1}^{M_{\alpha+s}} \Theta_1(\lambda_j^\alpha - \lambda_i^{\alpha+s}) - \sum_i^{M_\alpha} \Theta_2(\lambda_j^\alpha - \lambda_i^\alpha), \quad (2)$$

with $M_\alpha = \sum_{m=\alpha}^4 N_m$ ($M_0 = M_4 = 0$), where $\Theta_n(\lambda) = 2 \tan^{-1}(\cosh n\Phi \tan \frac{\lambda}{2})$. The quantum number $I_j^{(\alpha)}$ which specifies elementary excitations is subject to the constraints,

$$\begin{aligned} I_j^{(1)} &= \frac{1}{2}(M_1 + M_2) \pmod{1}, \\ I_j^{(2)} &= -\frac{1}{2}(M_1 - M_2 + M_3) \pmod{1}, \\ I_j^{(3)} &= \frac{1}{2}(M_2 - M_3) \pmod{1}. \end{aligned} \quad (3)$$

In the thermodynamic limit at zero temperature, the algebraic equations (2) are converted to the linear integral equations for the distribution functions of rapidities σ_α and for the dressed energies ε_α , respectively,^{25,34}

$$\begin{aligned} \varepsilon_\alpha(\lambda_\alpha) &= \varepsilon_\alpha^0(\lambda_\alpha) \\ &+ \sum_{\gamma=1}^3 \int_{-\lambda_\gamma^0}^{+\lambda_\gamma^0} \frac{d\lambda'_\gamma}{2\pi} K_{\alpha\gamma}(\lambda_\alpha - \lambda'_\gamma) \varepsilon_\gamma(\lambda'_\gamma), \end{aligned} \quad (4)$$

$$\begin{aligned} \sigma_\alpha(\lambda_\alpha) &= \sigma_\alpha^0(\lambda_\alpha) \\ &+ \sum_{\gamma=1}^3 \int_{-\lambda_\gamma^0}^{+\lambda_\gamma^0} \frac{d\lambda'_\gamma}{2\pi} K_{\alpha\gamma}(\lambda_\alpha - \lambda'_\gamma) \sigma_\gamma(\lambda'_\gamma), \end{aligned} \quad (5)$$

where $K_{\alpha\gamma} = -K_2\delta_{\alpha,\gamma} + K_1(\delta_{\alpha,\gamma+1} + \delta_{\alpha+1,\gamma})$, and $K_n(\lambda) = \sinh(n\Phi)/[\cosh(n\Phi) - \cos\lambda]$. Here, the bare distribution function is given by

$$\sigma_\alpha^0(\lambda_1) = \frac{1}{2\pi} K_1(\lambda_1) \delta_{\alpha 1}, \quad (6)$$

and ε_α^0 will be explicitly given separately for each case. The cut-off parameters ("Fermi level" for elementary excitations) λ_α^0 ($0 \leq \lambda_\alpha^0 \leq \pi$) are determined by minimizing the free energy for a given magnetic field, resulting in the condition,^{25,34} $\varepsilon_\alpha(\pm\lambda_\alpha^0) = 0$. For zero magnetic field, they are reduced to $\lambda_1^0 = \lambda_2^0 = \lambda_3^0 = \pi$. Since the dressed energies satisfy $\varepsilon_1(\pm\lambda_1^0 = \pi) = \varepsilon_2(\pm\lambda_2^0 = \pi) = \varepsilon_3(\pm\lambda_3^0 = \pi) < 0$, the system has three kinds of spin-gap excitations, which are degenerate at zero magnetic field.

As mentioned above, one of the most remarkable phenomena in 1D spin systems is the plateau formation in the magnetization,¹⁻⁵ which is regarded as a quantum phase transition driven by the magnetic field. Also, the middle-field cusp singularity³⁵ is another typical example of the field-induced quantum phase transition. In the following, we show that the multicomponent model (1) possesses a rich phase diagram in a magnetic field, where the magnetization has plateaus and/or cusps depending on the anisotropy as well as the Zeeman splitting. To demonstrate these things, we deal with two typical cases for which the energy splitting due to the magnetic field appears in different ways.

A. Spin-orbit multiplet case

We first assume that the Zeeman splitting is given by $g\mu_B M_z H$ with $M_z = \pm 1/2, \pm \gamma/2$, where γ ranges from 0 to 1. The corresponding Hamiltonian is

$$\mathcal{H}_{(A)} = -\frac{1}{2}h \sum_i [(n_{i,1/2} - n_{i,-1/2}) + \gamma(n_{i,\gamma/2} - n_{i,-\gamma/2})], \quad (7)$$

where $n_{i,\alpha}$ denotes the particle number for electrons with $M_z = \alpha$. Note that the case of $\gamma = 1/3$ corresponds to the Zeeman splitting for the spin-orbit multiplet $J_z = \pm 3/2, \pm 1/2$ ($M_z = \frac{1}{3}J_z$), while for $\gamma = 1$, the Zeeman effect acts only on the spin sector, so that the four-fold multiplet splits into two orbitally-degenerate levels in magnetic fields. The Zeeman term (7) may be applied to more generic cases including these two important cases. For example, in some Ce compounds such as CeB₆ the four-fold ground multiplet (Γ_8 multiplet) is generated in a cubic crystalline field under strong spin-orbit coupling. In such cases, the value of γ is known to depend on the strength of the crystalline field. We thus regard γ as a continuously changing parameter in the following discussions. We define the magnetization in terms of the distribution functions,

$$\begin{aligned} m_{(A)} &= \{(N_{1/2} - N_{-1/2}) + \gamma(N_{\gamma/2} - N_{-\gamma/2})\} / L \\ &= 1 - 2\gamma \int_{-\lambda_2^0}^{+\lambda_2^0} \sigma_2(\lambda_2) d\lambda_2 \\ &- (1 - \gamma) \left\{ \int_{-\lambda_1^0}^{+\lambda_1^0} \sigma_1(\lambda_1) d\lambda_1 + \int_{-\lambda_3^0}^{+\lambda_3^0} \sigma_3(\lambda_3) d\lambda_3 \right\}, \end{aligned} \quad (8)$$

where we have set the number of electrons as $N_1 = N_{1/2}, N_2 = N_{\gamma/2}, N_3 = N_{-\gamma/2}$ and $N_4 = N_{-1/2}$, respectively. Here ε_α^0 in (4) is given as

$$\begin{pmatrix} \varepsilon_1^0 \\ \varepsilon_2^0 \\ \varepsilon_3^0 \end{pmatrix} = \begin{pmatrix} -\sinh\Phi K_1(\lambda_1) + \frac{1}{2}(1 - \gamma)h \\ \gamma h \\ \frac{1}{2}(1 - \gamma)h \end{pmatrix}. \quad (9)$$

We have performed the calculation by iterating eq.(4) to determine the cutoff parameter λ_γ^0 for a given magnetic field, and then have evaluated the magnetization by solving eq.(5). Let us start with the spin-orbit level scheme for the multiplet specified by the total angular momentum. In Figs. 1(a) and (b), the magnetization curve for $\gamma = 1/3$ is shown by choosing two different values of the anisotropy, $\Phi = 1.7$ and $\Phi = 1.5$. When the magnetic field is increased from zero, the magnetization starts to increase at the finite critical field with a square-root dependence. For $\Phi = 1.5$, the $m = 1/3$ plateau appears, which is followed by two cusps in higher magnetic fields. On the other hand for $\Phi = 1.7$, two plateaus appear at $m = 1/3$ and $m = 2/3$, and the cusp structures are not generated. We note that the formation of plateaus in the present model is different from the

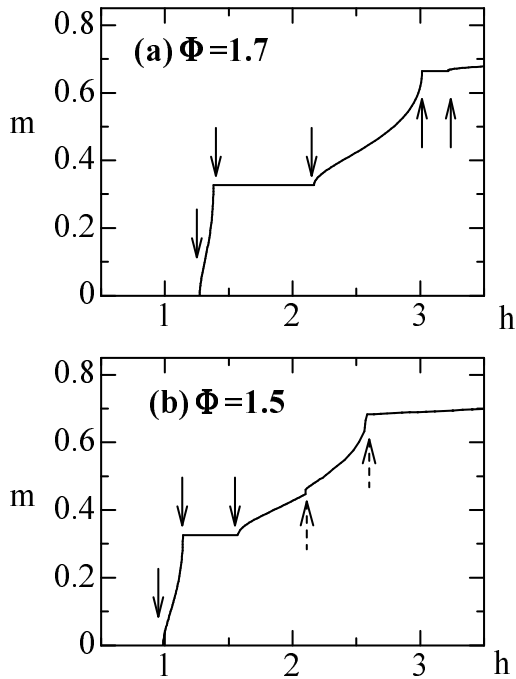


FIG. 1. The magnetization curve for (a) $\Phi = 1.7$ and (b) $\Phi = 1.5$: We denote the quantum phase transition points by the arrows. In particular, the positions of cusps are shown by the arrows with broken line. The saturated magnetization is $m = 1$.

standard fractional quantization discussed by Oshikawa *et al.*³, for which the plateau is stabilized by the spin-gap state that has magnetic order commensurate with the underlying lattice structure. On the other hand, in the present case, the plateau is generated when one of the multicomponent spin modes becomes massive, and the corresponding ground state is still in a disordered state which is not accompanied by the commensurate spin arrangement.

In Fig. 2, the $h - \Phi$ phase diagram is shown for the case of spin-orbit level scheme with $\gamma = 1/3$. Note that a massless mode exists in the regions I, II and III, in which the magnetization increases continuously with the field. In the area where two of I, II and III overlap with each other, there exist two massless modes. The cusp structure appears just at the boundary where these massless regions overlap. On the other hand, the regions of (a)-(d) outside of the massless regions denote the spin-gap phases, where the magnetization exhibits plateaus quantized as (a) $m = 0$, (b) $m = 1/3$, (c) $m = 2/3$, (d) $m = 1$, respectively. Note that the $\Phi = 0$ line corresponds to the isotropic SU(4) model,¹⁵ which is known to have only two cusps without plateaus.³⁵ The plateaus appear at $m = 1/3$ and $m = 2/3$ for sufficiently large Φ .

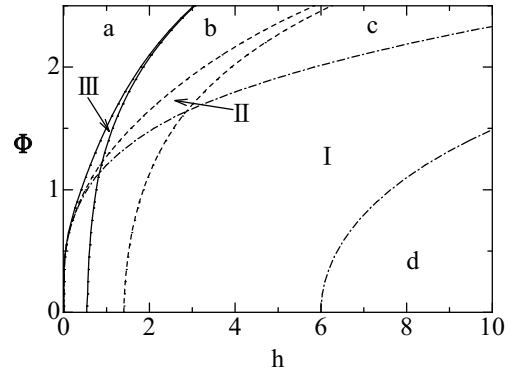


FIG. 2. The $h - \Phi$ phase diagram for the model (1) with (7) for $\gamma = 1/3$: The regions I, II and III denote the areas which are respectively sandwiched by two dash-dotted lines, two broken lines, and two solid lines, where each elementary excitation, ε_1 , ε_2 , or ε_3 is massless. Magnetization plateaus appear in the spin-gap phases outside of the above three regions: (a) $m = 0$, (b) $m = 1/3$, (c) $m = 2/3$, (d) $m = 1$. Magnetization cusps are observed at the boundary where two kinds of massless regions overlap.

For reference, we show in Fig. 3 the $h - \gamma$ phase diagram for $\Phi = 1.5$ to see how the scheme of the Zeeman splitting affects the magnetization curve. Recall that for the case of $\gamma = 1$, the four-fold degenerate states split into two-fold orbitally degenerate states in a magnetic field, for which the plateau-structure is absent. If the value of the parameter γ deviates from $\gamma = 1/3, 1$, the plateau appears at $m = (1 + \gamma)/2$ in the region (c).

B. Multiplet in a crystal field

We give another example of the magnetic phase diagram by employing a slightly different level scheme for which the orbital-splitting Δ due to the crystal field exists at zero magnetic field, and these two distinct levels further split in the presence of the magnetic field h . The corresponding Hamiltonian is

$$\mathcal{H}_{(B)} = \sum_i \left[-\frac{1}{2}h(n_{i,\uparrow} - n_{i,\downarrow}) - \Delta(n_{i,1} - n_{i,2}) \right], \quad (10)$$

where $n_{\uparrow} = n_{1\uparrow} + n_{2\uparrow}$ and $n_{\downarrow} = n_{1\downarrow} + n_{2\downarrow}$. The calculation of the magnetization is performed straightforwardly in the way outlined above. For $h \leq 2\Delta$, we set the number of electrons as $N_1 = N_{1\uparrow}, N_2 = N_{1\downarrow}, N_3 = N_{2\uparrow}$ and $N_4 = N_{2\downarrow}$, respectively. In this case, ε_{α}^0 is given by

$$\begin{pmatrix} \varepsilon_1^0 \\ \varepsilon_2^0 \\ \varepsilon_3^0 \end{pmatrix} = \begin{pmatrix} -\sinh \Phi K_1(\lambda_1) + h \\ -h + 2\Delta \\ h \end{pmatrix}. \quad (11)$$

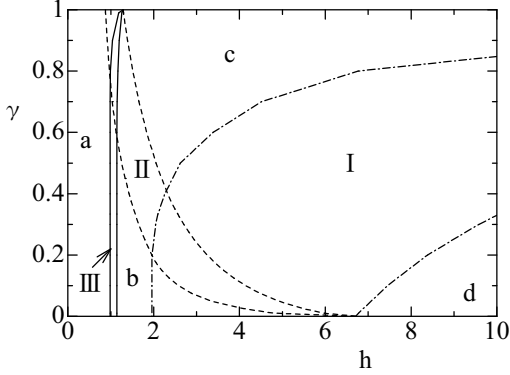


FIG. 3. The $h - \gamma$ phase diagram for the model (1) with (7) at $\Phi = 1.5$. Each region is specified following the way in Fig.2.

On the other hand, for $h \geq 2\Delta$, we set the number of electrons $N_1 = N_{1\uparrow}, N_2 = N_{2\uparrow}, N_3 = N_{1\downarrow}$ and $N_4 = N_{2\downarrow}$, for which ε_α^0 reads

$$\begin{pmatrix} \varepsilon_1^0 \\ \varepsilon_2^0 \\ \varepsilon_3^0 \end{pmatrix} = \begin{pmatrix} -\sinh \Phi K_1(\lambda_1) + 2\Delta \\ h - 2\Delta \\ 2\Delta \end{pmatrix}. \quad (12)$$

In Fig. 4, we show the $h - \Delta$ phase diagram derived for the anisotropy parameter $\Phi = 1.5$. Note that the phase diagram has two different regions labeled by II. This is because both the magnetic field and the crystal field play a similar role for the formation of the spin gap. The areas

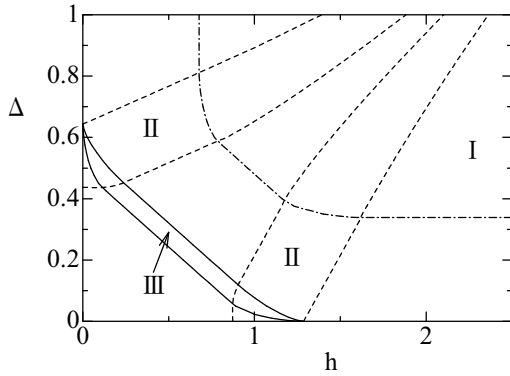


FIG. 4. The $h - \Delta$ phase diagram for Eqs. (1) and (10) at $\Phi = 1.5$. The meaning of massless regions I, II, III is same as in Fig.2. In the areas outside of these regions, the system is in a spin-gap phase.

outside of the regions I, II and III are all massive with the spin gap, as mentioned above. The mechanism for the formation of plateaus and cusps is as discussed before.

As summarized above, the multicomponent spin system with the spin gap exhibits interesting features such

as plateaus and cusps in the magnetization curve, depending on the anisotropy parameter.

III. NMR RELAXATION RATE

We have so far treated the static magnetization, and have shown that the quantum phase transitions are induced by the magnetic field, which are accompanied by the plateau and cusp singularities. It is then interesting to observe how dynamical quantities behave around such field-induced quantum phase transitions. To address this problem, we here study the NMR relaxation rate $1/T_1$ in magnetic fields with the emphasis on the behavior around plateaus and cusps.

The NMR relaxation rate for the multicomponent Tomonaga-Luttinger liquid is given at low temperatures by²⁶⁻²⁹

$$\begin{aligned} \frac{1}{T_1} &= \lim_{\omega \rightarrow 0} \frac{2k_B T}{\hbar^2 \omega} \int \frac{dk}{2\pi} A^2(k) \text{Im} \chi(k, \omega) \\ &\sim \sum_{\alpha} B_{\alpha} \Gamma_{\alpha}(h) T^{\eta_{\alpha}-1}, \end{aligned} \quad (13)$$

where

$$\Gamma_{\alpha}(h) = \left[\prod_{\mu} \left(\frac{1}{\tilde{v}_{\mu}} \right)^{2x_{\alpha\mu}} \right], \quad (14)$$

and B_{α} is a constant related to the hyperfine coupling, which is assumed to be independent of the temperature and the magnetic field. The above power-law dependence in temperature is typical for correlation functions in the Tomonaga-Luttinger liquid.³⁶ Since we are now dealing with the multicomponent system, there are several kinds of relaxation processes, providing different critical exponents η_{α} , where the index α classifies elementary excitations, e.g. $2k_F$ -current excitation, etc. To determine η_{α} , we should further incorporate the interference between different excitation modes,²⁹ which are explicitly expressed as $\eta_{\alpha} = \sum_{\mu} 2x_{\alpha\mu}$, where $x_{\alpha\mu}$ is the scaling dimension originating from the interference between α and μ modes. This formula can be straightforwardly obtained by analyzing the excitation spectrum in terms of finite-size scaling techniques in conformal field theory.³⁷⁻⁴¹

In the above formula, we have explicitly written down the factor (14) depending on the renormalized velocities \tilde{v}_{μ} , which have been usually neglected in the discussion of the temperature dependence of $1/T_1$. However, in order to study the field-dependence of $1/T_1$, we should take into account this factor, since it plays a crucial role around the critical points, as will be shown momentarily. We will refer to this factor as the enhancement factor in the following discussions.

Note that if the NMR is done on the nucleus of lattice spin, the relaxation occurs through a contact interaction and thereby $1/T_1$ depends only on the transverse susceptibility χ_{\perp} . On the other hand, if it is done on other

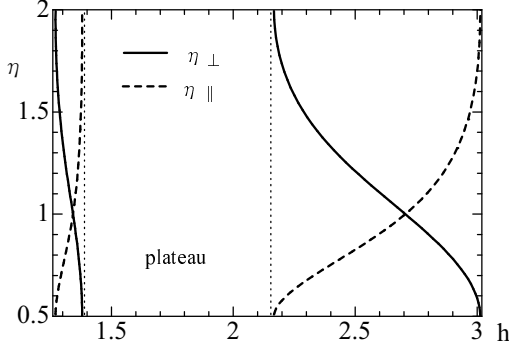


FIG. 5. Critical exponents around the $m = 1/3$ plateau in Fig. 1(a). The solid lines denote the most relevant critical exponents for the transverse spin susceptibility while the broken lines that for the longitudinal susceptibility.

neighboring nuclei, the relaxation is through dipolar interactions, and thus $1/T_1$ depends not only on χ_\perp but also on the longitudinal susceptibility χ_\parallel . In order to treat generic cases, we take into account the contributions both from χ_\perp and χ_\parallel . In the following, we discuss the critical properties of $1/T_1$ around plateaus and cusps.

A. Around the plateau

We start our discussion with the massless regions close to the magnetization plateau. For instance, we look at the critical region beside the $m = 1/3$ plateau in Fig. 1(a), where only one massless mode exists both in the left-hand side (III) and the right-hand side (II). In the region III, the scaling dimension x is obtained in a standard form via finite-size scaling analysis,³⁷

$$x = \frac{1}{4\xi_3^2} \Delta M^2 + \xi_3^2 \Delta D^2, \quad (15)$$

where so-called dressed charge³⁸ $\xi_3 = \lim_{\lambda_3 \rightarrow \lambda_3^0} \xi_3(\lambda_3)$ is determined by

$$\xi_3(\lambda_3) = 1 - \int_{-\lambda_3^0}^{+\lambda_3^0} \frac{d\lambda_3'}{2\pi} K_2(\lambda_3 - \lambda_3') \xi_3(\lambda_3'). \quad (16)$$

Here ΔM (ΔD) is the quantum number which changes the number of spinons (carries the $2k_F$ current). For the longitudinal spin susceptibility χ_\parallel the most relevant critical exponent is given by $\eta_\parallel = 2x = 2\xi_3^2$ by choosing $\Delta M = 0$ and $\Delta D = 1$, while for the transverse spin susceptibility χ_\perp , it is given by $\eta_\perp = \frac{1}{2}\xi_3^{-2}$ for $\Delta M = 1$ and $\Delta D = 0$. The critical exponents in region II can be obtained via a similar analysis.

In Fig. 5, we show the computed critical exponents as a function of the magnetic field h . Note that when the

critical exponents are smaller (larger) than unity, $1/T_1$ diverges (vanishes) with power-law dependence as the temperature decreases (see (13)). Similar behaviors can be found for the one-component spin-gap system studied by Chitra and Giamarchi.²⁸ We here pay our attention to the enhancement factor Γ_α at sufficiently low temperatures. In Fig. 6, we show Γ_\perp for the most relevant sector in the transverse susceptibility as a function of the magnetic field. We note that Γ_\parallel and Γ_\perp exhibit essentially the same critical behaviors. It is seen that $1/T_1$ is considerably enhanced in the vicinity of the plateau according to the dramatic renormalization of the velocities in the vicinity of the spin-gap phase. The enhancement of the relaxation rate is observed whenever the system is in a massless phase close to the spin-gap phase. For example, the relaxation rate is enhanced when the magnetization decreases to zero before forming the zero-field spin gap.

B. Around the cusp

Let us now observe what happens for $1/T_1$ around the cusp structure in the magnetization. We first look at the cusp at $h \simeq 2.1$ in Fig. 1(b). The critical behavior in the left-hand side of the cusp is described in terms of a massless mode. Therefore, this region can be analyzed following the way done for the plateau case. We thus have the enhancement of $1/T_1$ near the cusp. On the other hand, on the right-hand side of the cusp, two massless modes appear which need a different treatment for their critical properties. According to the conformal field theory analysis of multicomponent cases, the scaling dimension is given by the matrix form,³⁸⁻⁴¹

$$x = \frac{1}{4} \Delta \mathbf{M}^T (\boldsymbol{\xi}^{-1})^T (\boldsymbol{\xi}^{-1}) \Delta \mathbf{M} + \Delta \mathbf{D}^T \boldsymbol{\xi}^T \boldsymbol{\xi} \Delta \mathbf{D}, \quad (17)$$

where the quantum numbers in the vector representation are $\Delta \mathbf{M} = (\Delta M_1, \Delta M_2)^T$ and $\Delta \mathbf{D} = (\Delta D_1, \Delta D_2)^T$, which are subject to the selection rules,

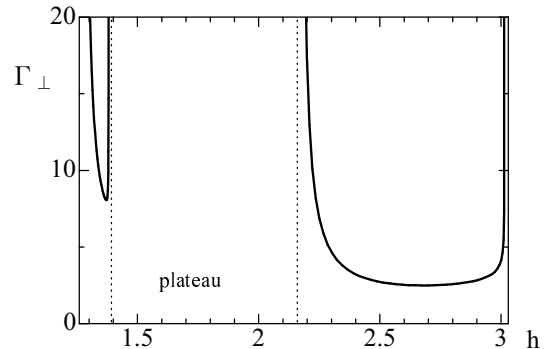


FIG. 6. The enhancement factor Γ_\perp around the plateau, $m = 1/3$, in the magnetization curve.

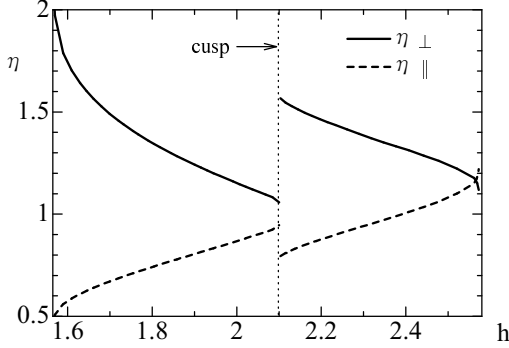


FIG. 7. The critical exponents around the cusp. As an example, we show them for the cusp of $h \simeq 2.1$ in Fig. 1(b).

$$\Delta D_1 = \frac{1}{2} \Delta M_2 \bmod 1, \quad \Delta D_2 = \frac{1}{2} \Delta M_1 \bmod 1. \quad (18)$$

Here the 2×2 dressed charge matrix³⁸ ξ has the elements $\xi_{\alpha\beta} = \xi_{\alpha\beta}(\lambda_\beta^0)$ which are determined by

$$\xi_{\alpha\beta}(\lambda_\beta) = \delta_{\alpha\beta} + \sum_{\gamma=1,2} \int_{-\lambda_\gamma^0}^{+\lambda_\gamma^0} \frac{d\lambda'_\gamma}{2\pi} K_{\beta\gamma}(\lambda_\beta - \lambda'_\gamma) \xi_{\alpha\gamma}(\lambda'_\gamma), \quad (19)$$

where $\alpha, \beta, \gamma = 1, 2$, and $K_{11}(\lambda) = K_{22}(\lambda) = -K_2(\lambda)$, $K_{12}(\lambda) = K_{21}(\lambda) = K_1(\lambda)$.

According to ref.⁴⁰, by properly choosing the set of quantum numbers $(\Delta M_1, \Delta M_2, \Delta D_1, \Delta D_2)$, we can determine the most relevant critical exponents. For χ_{\parallel} , we set $(0, 0, -1, 0)$, $(0, 0, -1, -1)$ and $(0, 0, 0, -1)$, because there is no change in the z -component of spin ($\Delta M_1 = \Delta M_2 = 0$), while for χ_{\perp} , we set $(-1, 0, 0, +\frac{1}{2})$, $(-1, -1, -\frac{1}{2}, +\frac{1}{2})$ and $(0, -1, -\frac{1}{2}, 0)$. In Fig. 7. the most relevant critical exponents obtained for χ_{\perp} and χ_{\parallel} are shown as a function of the magnetic field. It is seen that the critical exponent η_{\parallel} is smaller than η_{\perp} in a wide range of magnetic fields, which implies that χ_{\parallel} is dominant for the relaxation. As mentioned before, when the dipolar interactions are weak, A_{\parallel} should be nearly zero, so that the divergent behavior in $1/T_1$ may be masked at low temperatures in that case. On the other hand, the divergent behavior should be always observed around the plateaus, at least either on the right or left region. Fig. 8 shows the results for the enhancement factor Γ_{\perp} around the cusp in the magnetization. In contrast to the case of the plateau, the enhancement of $1/T_1$ appears on either side of the cusp, because Γ_{α} is enhanced when one of the massless modes becomes massive as the magnetic field is changed. For example, in the case of $\Phi = 0$ in Fig. 2, we have several quantum phase transition points at $h \simeq 0.54, 1.4, 6.0$, for which we can observe the enhancement of $1/T_1$ in the left-hand side of these points.

We have so far mentioned the enhancement of $1/T_1$ around plateaus and cusps in the magnetization. It is

noted here that such enhancement of $1/T_1$ is induced not only by the magnetic field but also by the orbital splitting. For instance, in Fig. 4, the relaxation rate for $h = 0$ is enhanced near the both edges of region II, when the orbital splitting Δ is continuously changed.

IV. SUMMARY

We have studied the magnetization process as well as the spin dynamics through the NMR relaxation rate for the 1D multicomponent spin-gap system. By using the solvable model of Bariev *et al*, we have found that the plateaus and the cusps are generated in the magnetization curve. We have also studied the NMR relaxation rate $1/T_1$ near plateaus and cusps in the magnetization. For the critical region around the plateau, $1/T_1$ diverges at low temperatures at least on either side of the plateau, whereas for the critical regions around the cusp, it depends on the values of the hyperfine coupling constants whether such a divergent behavior appears or not. It has also been found that the relaxation rate at low temperatures is enhanced near the critical value of the magnetic field. This is not only the case for the multicomponent model but also for ordinary spin chain models in magnetic fields. The enhancement appears at sufficiently low temperatures, so that it may be observed in rather ideal 1D spin systems for which the long-range order due to 3D dimensionality is suppressed even at low temperatures. Also, to extract this enhancement effect from the experimental data, careful analysis of the NMR data may be needed: e.g. the power-law temperature dependence should be determined precisely to obtain the correct coefficient as a function of the magnetic field. Although such an enhancement has not been observed yet for a typical 1D spin-1/2 system CuHpCl,³¹ we hope that more detailed experiments near the critical magnetic field may reveal the enhancement effect discussed here.

Although we have studied a rather specific integrable

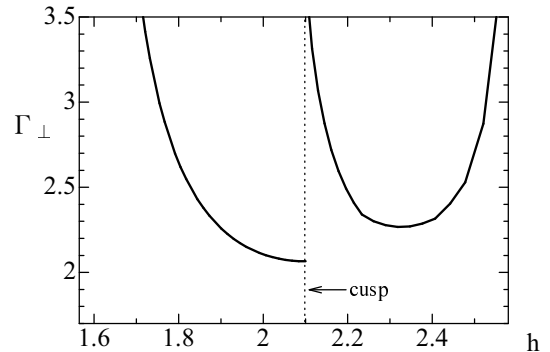


FIG. 8. The enhancement factor Γ_{\perp} for χ_{\perp} around the cusp in Fig. 1(b).

model, some characteristic features found in this paper are expected to hold for more generic 1D multicomponent quantum spin systems. In this connection, we note here that the $SU(2) \times SU(2)$ deformation of the massless $SU(4)$ model drives the system to a massive phase with spin gaps for all the excitation modes, according to recent intensive studies.^{20–24} We think that the characteristic features obtained in the present study can be also applied to the static and dynamical properties in this model.

ACKNOWLEDGEMENTS

This work was partly supported by a Grant-in-Aid from the Ministry of Education, Science, Sports and Culture of Japan. A. K. and F. T. were supported by Japan Society for the Promotion of Science. We would like to thank M. Sigrist for careful reading of the manuscript.

-
- ¹ K. Hida, J. Phys. Soc. Jpn. **63**, 2359 (1994).
² K. Okamoto, Solid. State. Commun. **98**, 245 (1995).
³ M. Oshikawa, M. Yamanaka and I. Affleck, Phys. Rev. Lett. **78**, 1984 (1997).
⁴ Y. Narumi, *et al.*, Physica B **246-247**, 509 (1998).
⁵ W. Shiramura, *et al.*, J. Phys. Soc. Jpn. **67**, 1548 (1998); Concerning the 3D effect, see A. K. Kolezhuk, Phys. Rev. B **59**, 4181 (1999) and the references therein.
⁶ V. Gedet, *et al.*, Phys. Rev. B **44**, 705 (1991).
⁷ G. Chaboussant *et al.*, Phys. Rev. B **55**, 3046 (1997).
⁸ E. Axtell, T. Ozawa, S. Kauzlarich and R. R. P. Singh, J. Solid. Chem. **134**, 423 (1997).
⁹ M. Isobe and Y. Ueda, J. Phys. Soc. Jpn. **65**, 1178 (1996); Y. Fujii *et al.*, J. Phys. Soc. Jpn. **66**, 326 (1997).
¹⁰ H. Seo and H. Fukuyama, J. Phys. Soc. Jpn. **67**, 2602 (1998).
¹¹ P. Thalmeier and P. Fulde, Europhys. Lett. **44**, 242 (1998).
¹² S. Nishimoto and Y. Ohta, J. Phys. Soc. Jpn. **67**, 2996 (1998).
¹³ Y. Yamashita, N. Shibata, and K. Ueda, Phys. Rev. B **58**, 9114(1998).
¹⁴ B. Frischmuth, F. Mila, M. Troyer, Phys. Rev. Lett. **82**, 835 (1999).
¹⁵ B. Sutherland, Phys. Rev. B **12**, 3795 (1975).
¹⁶ I. Affleck, Nucl. Phys. B **265**, 409 (1986).
¹⁷ T. Itakura and N. Kawakami, J. Phys. Soc. Jpn. **64**, 2321 (1995).
¹⁸ T. Fujii, Y. Tsukamoto and N. Kawakami, J. Phys. Soc. Jpn. **68**, 151 (1999).
¹⁹ Y. Q. Li, M. Ma, D. N. Shi and F. C. Zhang, Phys. Rev. B **60**, 12781 (1999).
²⁰ S. K. Pati and R. R. P. Singh, Phys. Rev. Lett. **81**, 5406 (1998).
²¹ P. Azaria, A. O. Gogolin, P. Lecheminant and A. A. Nersisyan, Phys. Rev. Lett. **83**, 624 (1999).
²² Y. Yamashita, N. Shibata, and K. Ueda: cond-mat/9908237.
²³ C. Itoi, S. Qin and I. Affleck: cond-mat/9910109.
²⁴ Y. Tsukamoto, N. Kawakami, Y. Yamashita and K. Ueda, Physica B in press.
²⁵ R. Z. Bariev, A. Klümper, A. Schadschneider and J. Zittarz Z. Phys. B **96**, 395 (1995).
²⁶ H. J. Schulz, Phys. Rev. B **34**, 6372 (1986).
²⁷ S. Sachdev, Phys. Rev. B **50**, 13 006 (1994).
²⁸ R. Chitra and T. Giamarchi, Phys. Rev. B **55**, 5816 (1997).
²⁹ A. Kawaguchi, T. Fujii and N. Kawakami (preprint).
³⁰ M. Takigawa, N. Motoyama, H. Eisaki and S. Uchida, Phys. Rev. Lett. **76**, 4612 (1996); Phys. Rev. B **56**, 13681 (1997).
³¹ G. Chaboussant *et al.*, Phys. Rev. Lett. **80**, 2713 (1998).
³² T. Goto *et al.*, Physica B in press.
³³ J. L. Cardy, Nucl. Phys. B **270**, 186 (1986).
³⁴ R. Sato, J. Phys. Condens. Matter **8**, 8363 (1996).
³⁵ K. Okunishi, Y. Hieida and Y. Akutu, Phys. Rev. B **60**, R6953 (1999).
³⁶ F. D. M. Haldane, Phys. Rev. Lett. **45**, 1358 (1980).
³⁷ N. M. Bogoliubov, A. G. Izergin and V. E. Korepin, Nucl. Phys. B **275**, 687 (1986); S. V. Pokrovskii and A. M. Tsvelik, Sov. Phys. JETP **66**, 1275 (1987).
³⁸ A. G. Izergin, V. E. Korepin and N. Yu. Reshetikhin, J. Phys. A **22**, 2615 (1989).
³⁹ F. Woynarovich, J. Phys. A **22**, 4243 (1989).
⁴⁰ H. Frahm and V. E. Korepin, Phys. Rev. B **42**, 10553 (1990).
⁴¹ N. Kawakami and S. K. Yang, Phys. Rev. Lett. **65**, 2309 (1990).